Inorganic Chemistry

Article

pubs.acs.org/IC

Aliphatic C−C Bond Cleavage of α-Hydroxy Ketones by Non-Heme Iron(II) Complexes: Mechanistic Insight into the Reaction Catalyzed by 2,4′-Dihydroxyacetophenone Dioxygenase

Rubina Rahaman, Sayantan Paria, and Tapan Kanti Paine*

Department of Inorganic Chemistry, Indian Association for the Cultivation of Science, 2A & 2B Raja S. C. Mullick Road, Jadavpur, Kolkata 700032, India

Supporting Information

ABSTRACT: 2,4′-Dihydroxyacetophenone dioxygenase (DAD) is a bacterial non-heme enzyme that carries out oxygenative aliphatic C−C bond cleavage of 2,4′-dihydroxyacetophenone (an α-hydroxy ketone) with the incorporation of both the oxygen atoms of dioxygen into the cleavage products. The crystal structure of the iron enzyme DAD has recently been determined, but very little is known about the mechanism of the C−C bond cleavage reaction. With the objective of gaining insights into the mechanism of the reaction catalyzed by DAD, six new biomimetic iron(II)-α-hydroxy ketone complexes, [(Tp^{Ph2})Fe^{II}(PHAP)] (**1**), [(Tp^{Ph2})Fe^{II}(HCH)] (**2**), [(Tp^{Ph2})Fe^{II}(HBME)] (**3**), [(Tp^{Ph2})Fe^{II}(CHPE)] (**4**), [(6-Me_3-TPA)Fe^{II}(PHAP)]$^+$ (**5**), and [(6-Me_3-TPA)Fe^{II}(HCH)]$^+$ (**6**) (Tp^{Ph2} = hydrotris(3,5-diphenylpyrazol-1-yl)borate, 6-Me_3-TPA = tris(6-methyl-2-pyridylmethyl)amine, PHAP-H = 2-phenyl-2-hydroxyacetophenone, HCH-H = 2-hydroxycyclohexanone, HBME-H = 2-hydroxy-1,2-bis(4-methoxyphenyl)ethanone, and CHPE-H = 1-(4-chlorophenyl)-2-hydroxy-2-phenylethanone), have been isolated and characterized. The single-crystal X-ray structure of **2** shows a five-coordinate iron(II) complex with one tridentate facial ligand and a monoanionic bidentate α-hydroxy ketone, resulting in a distorted-square-pyramidal coordination geometry at the iron center. The iron(II) complexes react with dioxygen to oxidatively cleave the aliphatic C−C bonds of the coordinated α-hydroxy ketones to afford 2 equiv of carboxylic acids. Mechanistic studies reveal that the C−C bond cleavage reaction proceeds through an intradiol pathway. Additionally, the coordinated α-hydroxy ketones in all of the complexes, except in complex **4**, undergo two-electron oxidation to form the corresponding 1,2-diketones. However, the yields of 1,2-diketones are higher with the iron complexes of the tripodal N_4 ligand (6-Me_3-TPA) in comparison to the facial N_3 ligand (Tp^{Ph2}). These results strongly support the natural selection of a facial N_3 environment at the active site of the iron enzyme DAD.

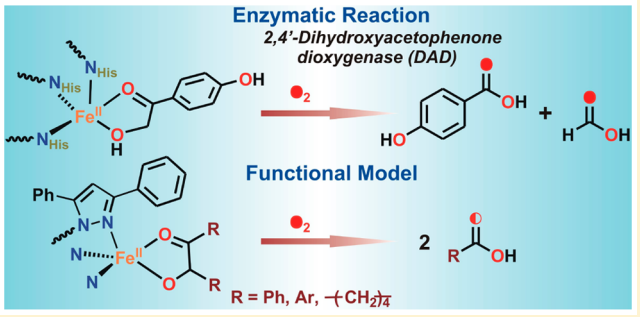

INTRODUCTION

Different microorganisms in soil and groundwater biodegrade various toxic chemicals and xenobiotics.[1,2] In the bacterial biodegradation pathway of 2,2-bis(4-hydroxyphenyl)propane (bisphenol A),[3−6] a small amount of 2,4′-dihydroxyacetophenone is formed as an end product which is not metabolized by bisphenol A-degrading bacterium.[7] 2,4′-Dihydroxyacetophenone dioxygenase (DAD), an enzyme isolated from the aerobic soil bacterium *Alcaligenes* sp. grown on 4-hydroxyacetophenone, catalyzes the cleavage of 2,4′-dihydroxyacetophenone into 4-hydroxy benzoate and formate under aerobic conditions with the incorporation of both oxygen atoms of O_2 into products (Scheme 1).[8−10] The enzyme does not show significant sequence homology to other known dioxygenases.[10,11] DAD has been reported to be a member of the cupin superfamily of enzymes and is a homotetramer containing iron in the active site.[11]

The isolation, purification, and catalytic reactivity of a DAD from *Burkholderia* Sp. AZ11 have recently been reported.[12]

Scheme 1. Reaction Catalyzed by DAD

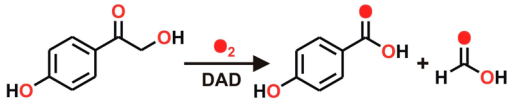

This enzyme has been reported to be a homotetramer containing 1.63−1.69 equiv of iron per mole of the enzyme. On the basis of optical spectral data of the enzyme and of the enzyme in the presence of substrate, binding of the substrate to the iron(III) center has been proposed. It has further been reported that the α-hydroxy ketone unit of the substrate was essential to exhibit enzymatic activity. A mechanism similar to that of intradiol catechol dioxygenases has been proposed for this enzyme.[12] However, in the absence of any strong spectroscopic evidence, the oxidation state of iron in the

Received: June 1, 2015

DOI: 10.1021/acs.inorgchem.5b01235
Inorg. Chem. XXXX, XXX, XXX−XXX

enzyme remains a speculation. Therefore, a detailed investigation is needed to establish the oxidation state of iron as well as its role in the C−C bond cleavage mechanism.

Biomimetic functional model complexes have been reported to provide valuable information in understanding the mechanism of the reactions catalyzed by aliphatic C−C bond cleaving oxygenases.[2,13−23] However, the model chemistry of DAD has not been developed well because of the absence of structural and detailed spectroscopic characterization of this enzyme. A number of crystallographic studies on this enzyme have been performed,[24] but until very recently the 3D structure of the enzyme was not known. In 2012, we reported a five-coordinate iron(II) complex of a facial tridentate ligand, $[(Tp^{Ph2})Fe^{II}(HAP)]$ (Tp^{Ph2} = hydrotris(3,5-diphenylpyrazol-1-yl)borate, HAP-H = 2-hydroxyacetophenone), as the first model complex of DAD.[25] The basis of using a facial N_3 ligand was to mimic the facial three-histidines motif observed in a crystallographically characterized cupin nonheme iron enzyme, gentisate 1,2-dioxygenase.[26] The complex has been shown to react with oxygen to cleave the aliphatic C−C bond of 2-hydroxyacetophenone to afford benzoic acid and formic acid quantitatively. A labeling experiment with $^{18}O_2$ suggests the incorporation of one ^{18}O atom (40% incorporation) into each of the products exhibiting typical dioxygenase type reactivity.[25] Very recently, Cooper and co-workers reported the X-ray diffraction data collected at a resolution of 2.2 Å at a synchrotron that allowed the first 3D structure determination of DAD from *Alcaligenes* sp.[27,28] The structure reveals that the catalytic iron is ligated by three histidines along with an additional ligand tentatively assigned as a dianionic carbonate. The additional ligand is proposed to be replaced by the α-hydroxy ketone substrate during catalysis.[28] The enzyme has been reported to contain ferrous iron in the active site. The model complex $[(Tp^{Ph2})Fe^{II}(HAP)]$ has several key features in common with the active site of the enzyme, including the coordination of an N_3 facial triad and bidentate binding of the α-hydroxy ketone to the iron(II) center.[25] Cooper and his group investigated the mechanism of the enzymatic reaction[28] on the basis of our proposal on the aliphatic C−C bond cleavage of 2-hydroxyacetophenone with dioxygen by the $Tp^{Ph2}Fe^{II}$ complex.

To gain further insight into the mechanism of the aliphatic C−C bond cleavage reaction by DAD, we have explored the reactivity of several iron(II)-α-hydroxy ketone complexes using nitrogen donor polydentate ligands. In this study, we used one facial N_3 and one tripodal N_4 ligand to evaluate the effect of ligand denticity in directing the C−C bond cleavage pathway. We report herein the synthesis and characterization of six new biomimetic iron(II)-α-hydroxy ketone complexes: $[(Tp^{Ph2})Fe^{II}(PHAP)]$ (**1**), $[(Tp^{Ph2})Fe^{II}(HCH)]$ (**2**), $[(Tp^{Ph2})Fe^{II}(HBME)]$ (**3**), $[(Tp^{Ph2})Fe^{II}(CHPE)]$ (**4**), $[(6\text{-}Me_3\text{-}TPA)Fe^{II}(PHAP)]^+$ (**5**), and $[(6\text{-}Me_3\text{-}TPA)Fe^{II}(HCH)]^+$ (**6**) (6-Me_3-TPA = tris(6-methyl-2-pyridylmethyl)amine, PHAP-H = 2-phenyl-2-hydroxyacetophenone, HCH-H = 2-hydroxycyclohexanone, HBME-H = 2-hydroxy-1,2-bis(4-methoxyphenyl)-ethanone, and CHPE-H = 1-(4-chlorophenyl)-2-hydroxy-2-phenylethanone) (Scheme 2). The reactivity of the complexes toward dioxygen and the mechanism of the oxidative C−C bond cleavage of coordinated α-hydroxy ketones on the iron(II) complexes are presented in this work.

RESULTS AND DISCUSSION

Synthesis and Characterization. The iron(II) complexes **1**−**6** were isolated from the reactions of equimolar amounts of ligand and iron(II) perchlorate hexahydrate with the respective monoanionic α-hydroxy ketone in methanol at room temperature (Scheme 2). The iron(II) complexes of 2-hydroxy-1,2-bis(4-methoxyphenyl)ethanone and 1-(4-chlorophenyl)-2-hydroxy-2-phenylethanone using the 6-Me_3-TPA ligand, however, could not be isolated in pure form. The isolated complexes are soluble in common organic solvents and are stable under a nitrogen atmosphere.

Scheme 2. Synthesis of Iron(II)-α-Hydroxy Ketone Complexes

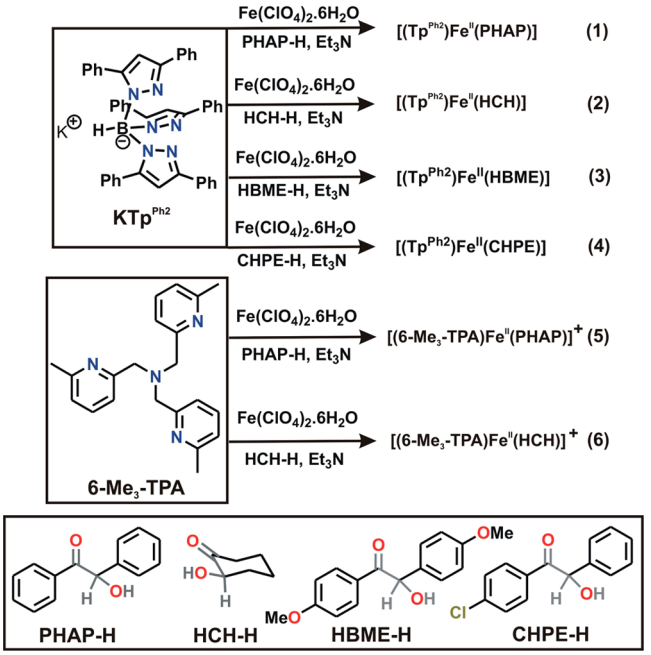

The optical spectrum of **1** is dominated by two absorption bands at 515 and 570 nm. These absorption bands arise from the charge-transfer (CT) transitions from the filled d orbital of the iron(II) to the empty π* orbital of the keto group of PHAP (Figure 1).[25] The CT bands shift slightly higher in energy to 500 and 555 nm upon introduction of electron-donating methoxy groups on the phenyl rings of α-hydroxy ketone in **3**.

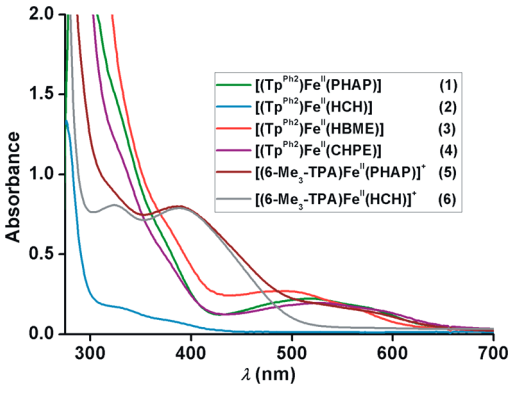

Figure 1. Optical spectra of iron(II)-α-hydroxy ketone complexes (0.5 mM in C_6H_6 for **1**−**4** and in CH_3CN for **5**−**6**) at 298 K.

DOI: 10.1021/acs.inorgchem.5b01235
Inorg. Chem. XXXX, XXX, XXX−XXX

For complex **4**, in which the α-hydroxy ketone contains one electron-withdrawing chloro group, the CT bands shift to lower energy at 530 and 580 nm. Although complex **2** displays similar absorption features, the CT bands are blue-shifted in comparison to those of **1**. The energy of the π^* orbital of keto group of the coordinated HCH is increased due to lack of conjugation (Figure 1). The UV−vis spectrum of **5** shows CT bands at around 560 nm similar to those of iron(II) α-keto acid complexes of N_4 donor ligands.[29] Another band at 390 nm in **5** may be attributed to CT transition from the filled d orbital of iron(II) to the π^* orbital of pyridine rings of the ligand.[29] These CT bands, however, get shifted to higher energy in complex **6** (Figure 1). The optical spectral data support the bidentate binding of α-hydroxy ketones to the metal center in keto forms. The ^{1}H NMR spectra exhibit paramagnetically shifted proton resonances of the ligands in the region between 80 and −40 ppm, indicating the high-spin nature of the iron(II) complexes (see the Experimental Section and Figures S1−S6 in the Supporting Information). Room-temperature magnetic moment values for the complexes are found to be in the range of 4.9−5.3 μ_B, typical of high-spin iron complexes with an S = 2 ground state. The analytical and spectroscopic data confirm the composition of the complexes (for ESI-MS, see Table S1 in the Supporting Information). Additionally, the presence of solvent molecules in the analytical samples of **1** and **2** was further confirmed by thermogravimetric analysis (TGA) (Figures S7 and S8 in the Supporting Information).

X-ray Crystal Structure. To assess the binding mode of α-hydroxy ketones to the iron center, attempts were made to grow single crystals of the complexes. While X-ray-quality single crystals of **2** were grown by layer diffusion of methanol into a dichloromethane solution of the complex at ambient temperature, other iron(II)-α-hydroxy ketone complexes could not be crystallized. Complex **2** crystallizes in the monoclinic system with $P2_1/c$ space group. The crystal structure of the neutral complex reveals a mononuclear five-coordinate iron center coordinated by three nitrogen donors from the monoanionic N_3 ligand and two oxygen donors of a bidentate 2-hydroxycyclohexanoate (HCH) ring (Figure 2). The iron−nitrogen bond distances are found in the range of 2.107(2)−2.193(2) Å, which are in good agreement with the only reported high-spin iron(II)-α-hydroxy ketone complex of the Tp^{Ph2} ligand (Table 1).[25]

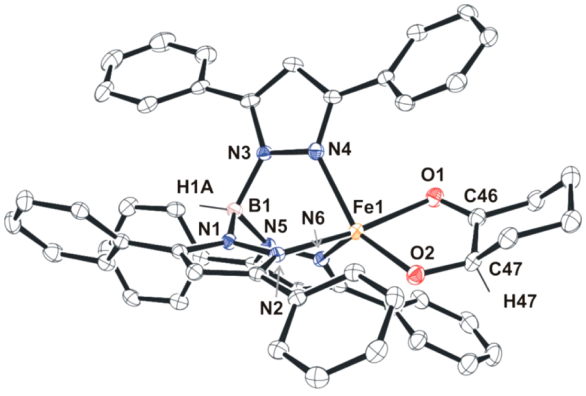

Figure 2. ORTEP plot of [(Tp^{Ph2})Fe^{II}(HCH)] (**2**) with 40% thermal ellipsoid parameters. All hydrogen atoms, except those on B1 and C47, have been omitted for clarity.

In the complex, HCH coordinates to the iron center in a bidentate mode through one carbonyl oxygen (O1) and one alcoholate oxygen (O2) with Fe1−O1 and Fe1−O2 distances of 2.281(2) and 1.916(2) Å, respectively (Table 1). The C46−O1 (1.227(4) Å), C47−O2 (1.394(4) Å), and C46−C47 (1.507(4) Å) distances indicate that HCH coordinates to the iron center in a keto form. The C−C and C−O bond distances of the coordinated α-hydroxy ketone in **2** are found to be very similar to those of the reported metal complexes with α-hydroxy ketone ligands, further confirming the monoanionic binding of HCH without enolization.[30−34] While the iron center in [(Tp^{Ph2})Fe^{II}(HAP)][25] adopts a distorted-trigonal-bipyramidal coordination geometry (τ = 0.62),[35] the iron center in **2** adopts a distorted-square-pyramidal coordination geometry (τ = 0.45). In the complex, the cyclohexane ring of HCH adopts a chair conformation where the keto and the alcoholate groups are positioned equatorially, enabling the α-hydroxy ketone to bind to the iron center in a bidentate fashion.

Reactions of Iron(II)-α-Hydroxy Ketone Complexes with Dioxygen. All of the iron(II) α-hydroxy ketone complexes are sensitive toward dioxygen. Exposure of a benzene solution of **1** to dioxygen at 10 °C results in a very rapid decay of the CT bands at 515 and 570 nm following pseudo-first-order kinetics (k_{obs} = [1.8(±0.6)] × 10^{-2} s^{-1} at 10 °C) (Figure 3a). The complex reacts with dioxygen ∼20 times faster than does the iron(II)-α-keto acid complex [(Tp^{Ph2})-Fe^{II}(benzoylformate)].[36] The faster reactivity of **1** could be attributed to an increased electron donating ability of the hydroxyl group.[37] Complex **2** reacts with O_2 in dry benzene at 10 °C for over 1 h (k_{obs} = [1.0(±0.8)] × 10^{-3} s^{-1} at 10 °C), during which time the CT bands at 330 and 380 nm disappear to produce a light yellow solution (Figure 3b). Complexes **3** and **4** exhibit similar optical spectral changes during the reaction with dioxygen, where the CT bands disappear following a pseudo-first-order rate equation with the respective k_{obs} values of [3.3(±0.3)] × 10^{-3} and [3.8(±0.3)] × 10^{-2} s^{-1} at 10 °C (Figure S9 in the Supporting Information).

The ESI-mass spectra of the oxidized solutions of all four complexes exhibit an ion peak at m/z 725.11 with an isotope distribution pattern attributable to [(Tp^{Ph2})Fe]$^+$ (Figure 3b, inset). In addition, the oxidized solution of **1** exhibits resonance signals similar to those of [(Tp^{Ph2})Fe^{II}(benzoate)][36] in the ^{1}H NMR spectrum (Figure S10 in the Supporting Information). During the reaction, intramolecular ligand hydroxylation is not observed, but the resulting iron(II)-benzoate complex, as reported earlier,[36] slowly reacts with dioxygen to afford intramolecular oxygenated complex. Other complexes, after the reaction with dioxygen, also exhibit paramagnetically shifted proton resonances typical of a high-spin iron(II) complex of Tp^{Ph2} (Figure S11 in the Supporting Information). Moreover, the final oxidized solutions of **1**, **2**, and **4** are X-band EPR silent at 77 K. Therefore, the iron(II)-α-hydroxy ketone complexes undergo oxidative transformation to form the corresponding iron(II)-carboxylate products. In the reaction, no decomposition of the supporting ligand is observed.

The organic products from each of the oxidized solutions of **1**−**4**, after separation of the metal ion by acidic workup, were analyzed by GC-MS and ^{1}H NMR spectroscopy. In the case of **1**, PHAP is oxidized to a mixture of benzoic acid (85(±3)%) and benzil (12(±3)%) (Table 2, Figure 4, and Scheme 3), and for **2**, 85(±3)% adipic acid and 13(±2)% cyclohexane-1,2-dione are formed from HCH (Table 2 and Figure 5). Complex

DOI: 10.1021/acs.inorgchem.5b01235
Inorg. Chem. XXXX, XXX, XXX−XXX

Table 1. Selected Bond Lengths (Å) and Angles (deg) for [(Tp^{Ph2})Fe^{II}(HCH)] (2)

Fe(1)−N(2)	2.193(2)	C(46)−O(1)	1.227(4)
Fe(1)−N(4)	2.107(2)	C(47)−O(2)	1.394(4)
Fe(1)−N(6)	2.119(2)	C(46)−C(47)	1.507(4)
Fe(1)−O(1)	2.281(2)	Fe(1)−O(2)	1.916(2)
N(4)−Fe(1)−O(1)	94.10(8)	O(2)−Fe(1)−O(1)	78.18(8)
N(4)−Fe(1)−O(2)	121.32(9)	O(2)−Fe(1)−N(2)	104.03(9)
N(4)−Fe(1)−N(2)	90.65(9)	N(6)−Fe(1)−N(2)	83.27(9)
N(4)−Fe(1)−N(6)	91.69(9)	N(6)−Fe(1)−O(1)	91.03(8)
N(2)−Fe(1)−O(1)	172.69(8)	N(6)−Fe(1)−O(2)	145.60(9)

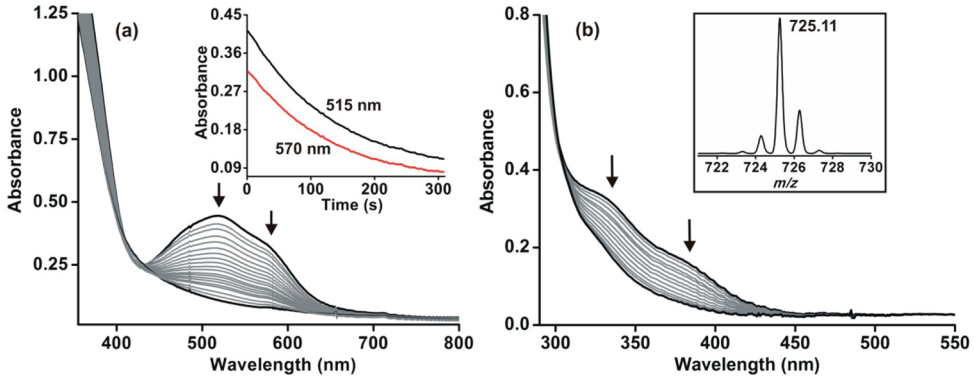

Figure 3. UV−vis spectral changes of (a) complex **1** and (b) complex **2** (1 mM in benzene) during the reaction with dioxygen at 283 K. Insets: (a) absorbance as a function of time; (b) ESI-mass spectrum of the oxidized solution of **2**.

Table 2. Percentages of Different Oxidation Products Derived from α-Hydroxy Ketones

complex	C−C cleavage product (%)	1,2-diketone product (%)	unreacted product (%)	conversion of α-hydroxy ketone (%)
[(Tp^{Ph2})Fe^{II}(PHAP)] (**1**)	85(±3)	12(±3)	0	97
[(Tp^{Ph2})Fe^{II}(HCH)] (**2**)	85(±3)	13(±2)	0	98
[(Tp^{Ph2})Fe^{II}(HBME)] (**3**)	76(±2)	18(±2)	2(±2)	94
[(Tp^{Ph2})Fe^{II}(CHPE)] (**4**)	quantitative		0	quantitative
[(6-Me$_3$-TPA)Fe^{II}(PHAP)]BPh$_4$ (**5**)	38(±3)	53(±3)	9(±3)	91
[(6-Me$_3$-TPA)Fe^{II}(HCH)]BPh$_4$ (**6**)	55(±3)	37(±1)	8(±3)	92
[(Tp^{Ph2})Fe^{II}(HAP)][a]	quantitative		0	quantitative

[a]Reference 25.

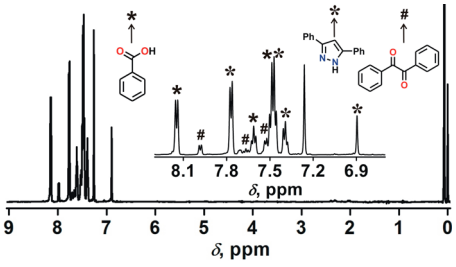

Figure 4. ^{1}H NMR (500 MHz, $CDCl_3$, 295 K) spectrum of organic products isolated from the oxidized solution of [(Tp^{Ph2})Fe^{II}(PHAP)] (**1**).

Scheme 3. C−C Bond Cleavage Products of α-Hydroxy Ketones on the Iron(II) Complexes

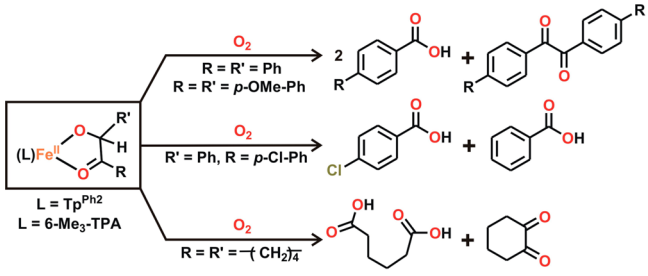

3 affords *p*-methoxybenzoic acid (76(±2)%) and 1,2-bis(4-methoxyphenyl)ethane-1,2-dione (18(±2)%) (Table 2 and Figure S12 in the Supporting Information). In contrast, complex **4** yields *p*-chlorobenzoic acid (52(±2)%) and benzoic acid (48(±2)%) without any diketone (Table 2, Scheme 4, and Figure S13 in the Supporting Information). The formation of adipic acid from **2** was also confirmed by ^{13}C NMR spectroscopy (Figure S14 in the Supporting Information). It is important to mention here that neither the C−C bond cleavage product (benzoic acid or adipic acid) nor the diketone is observed in control experiments with equimolar amounts of iron(II) salt and α-hydroxy ketones. In the control experiments, however, addition of triethylamine to the reaction mixture results in the formation of about 25−30% of dione products without any C−C bond cleavage product.

Adipic acid obtained from the oxidized solution of **2** was esterified for further analysis. In the ^{1}H NMR spectrum, the phenacyl ester of adipic acid exhibits three sets of methylenic protons (Figure S15 in the Supporting Information). The ESI-mass spectrum of the ester displays molecular ion peaks at *m*/*z*

DOI: 10.1021/acs.inorgchem.5b01235
Inorg. Chem. XXXX, XXX, XXX−XXX

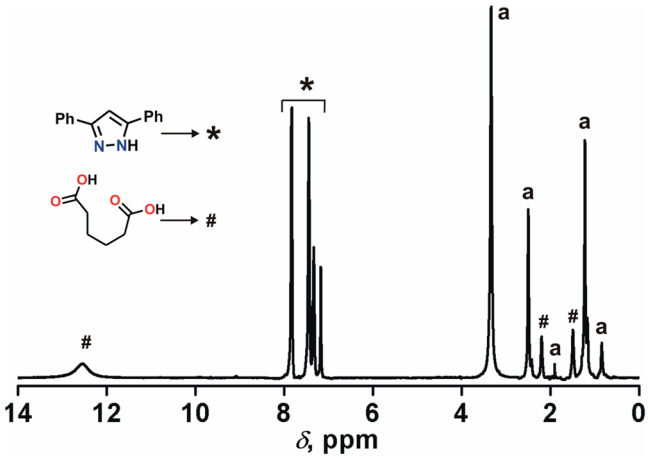

Figure 5. ^{1}H NMR (300 MHz, DMSO-d_6, 295 K) spectrum of 2-hydroxycyclohexanone-derived product after the reaction of [(Tp^{Ph2})-Fe^{II}(HCH)] (**2**) with dioxygen. Peaks marked with "a" are from residual solvents.

Scheme 4. Reactivity of the α-Hydroxy Ketones That Do Not Contain Any α-C−H Bond

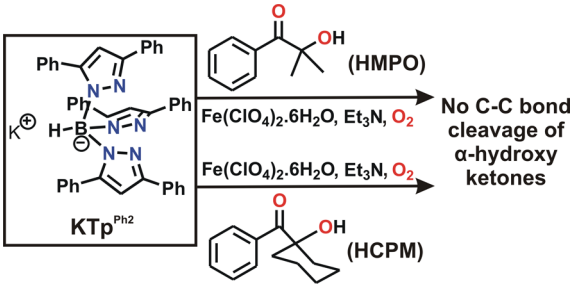

421.16 and 405.16 for $[C_{22}H_{22}O_6 + K]^+$ and $[C_{22}H_{22}O_6 + Na]^+$, respectively, along with the expected fragmentation patterns, confirming the formation of adipic acid in the oxidative C−C bond cleavage of HCH (Figure S16 in the Supporting Information).

The dioxygen reactivity of the iron(II) complexes (**5** and **6**) of the tetradentate ligand is slow compared to that of the complexes (**1**−**4**) of the tridentate ligand. An acetonitrile solution of **5** reacts with dioxygen over a period of 3 h (k_{obs} = [3.9(±0.8)] × 10^{-4} s^{-1} at 25 °C), during which the brown solution turns yellow. In the reaction, the CT bands at 390 and 560 nm decay slowly (Figure 6a). The reaction of **6** with dioxygen takes about 6 h with a k_{obs} value of [1.5(±0.3)] × 10^{-6} s^{-1} at 25 °C (Figure 6b). The ESI-mass spectrum of the oxidized solution of **5** displays an ion peak at m/z 509.02 with the isotope distribution pattern calculated for [(6-Me$_3$-TPA)-Fe^{II}(benzoate)]$^+$ (Figure 6a, inset). The ^{1}H NMR spectrum of the solution also matches with that of the reported [(6-Me$_3$-TPA)Fe^{II}(benzoate)]$^+$ complex (Figure S17 in the Supporting Information).[38] Additionally, the X-band EPR spectrum (at 77 K) of the oxidized solution of **5** shows a weak signal at g = 4.2 typical of a high-spin iron(III) complex. Thus, in addition to the paramagnetic benzoate complex, the oxidized solution of **5** contains other iron species that could not be characterized (Figure S17 (inset)).

Analyses of organic products from **5** and **6** reveal that the percentage of oxidative C−C bond cleavage is low; the corresponding 1,2-diketones are formed in higher amounts. While complex **5** affords 38(±3)% benzoic acid and 53(±3)% benzil (Figure S18 in the Supporting Information), complex **6** yields 55(±3)% adipic acid and 37(±1)% cyclohexane-1,2-dione (Scheme 3 and Table 2). In both cases, about 8−9% of the α-hydroxy ketone remains unreacted.

The α-hydroxy ketones discussed above contain one α-C−H bond. To establish the role of the α-C−H bond in the C−C bond cleavage, attempts were made to isolate iron(II) complexes of the α-hydroxy ketones that do not contain an α-C−H bond. Unfortunately, the iron complex of 2-hydroxy-2-methyl-1-phenylpropane-1-one (HMPO) or 1-hydroxycyclohexyl-1-phenylmethanone (HCPM) could not be isolated. The reaction of equimolar amounts of the ligand KTp^{Ph2}, iron(II) perchlorate, HMPO (or HCPM), and triethylamine with dioxygen in a benzene/methanol (9/1) solvent mixture does not produce any C−C bond cleavage product (Scheme 4 and Figures S19 and S20 in the Supporting Information). On the other hand, reactions involving mixtures of nitrogen donor ligand, iron(II) salt, base, dioxygen, and α-hydroxy ketones containing one α-H atom lead to a mixture of the C−C cleavage products and diketones, although the yields of oxidized products (30−40% overall) are found to be less than those involving isolated complexes and dioxygen. These results therefore support that the presence of a C−H bond in α-hydroxy ketone is essential for the oxygen-dependent C−C bond cleavage reaction.

Mechanistic Studies. To gain an understanding of the mechanism of the C−C bond cleavage reactions of α-hydroxy ketones, isotope labeling experiments were performed. The

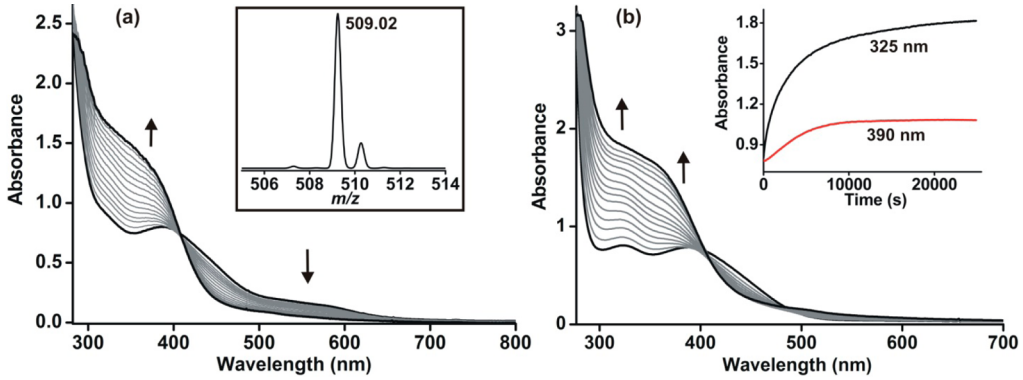

Figure 6. Optical spectral changes of (a) **5** and (b) **6** (0.5 mM in acetonitrile) during the reaction with dioxygen at 298 K. Insets: (a) isotope distribution pattern in the ESI-mass spectrum of the oxidized solution of **5**; (b) absorption intensity as a function of time for **6**.

DOI: 10.1021/acs.inorgchem.5b01235
Inorg. Chem. XXXX, XXX, XXX−XXX

Table 3. Incorporation of Labeled Oxygen Atoms from $^{18}O_2$ and $H_2{}^{18}O$ into the Oxidized Products of α-Hydroxy Ketones

	^{18}O atom incorporated into C−C cleavage product (%)		^{18}O atom incorporated into diketone product (%)	
complex	from $^{18}O_2$	from $H_2{}^{18}O$	from $^{18}O_2$	from $H_2{}^{18}O$
$[(Tp^{Ph2})Fe^{II}(HAP)]$	40[a]	5[b]	not applicable	not applicable
$[(Tp^{Ph2})Fe^{II}(PHAP)]$ (**1**)	55[b]	15[b]	0	not determined
$[(Tp^{Ph2})Fe^{II}(HCH)]$ (**2**)	47[b]	10[b]	0	25[c]
$[(6\text{-}Me_3\text{-}TPA)Fe^{II}(PHAP)]^+$ (**5**)	70[d]	20[d]	0	10[c]

[a]Reference 25. [b]Quantified by GC-MS of the ester of carboxylic acids. [c]Quantified by GC-MS. [d]Quantified by ESI-MS (positive ion mode in acetonitrile) of the carboxylate-coordinated metal complex.

GC-mass spectrum of methyl ester of the benzoic acid obtained from the reaction between **1** with $^{18}O_2$ shows around 55% incorporation of one ^{18}O atom into benzoate, where the ion peak at m/z 136 shifts to 138 (Table 3 and Figure S21a,b in the Supporting Information). Additionally, a small peak observed at m/z 140 indicates the incorporation of two labeled oxygen atoms into benzoate (Figure S21b). In a mixed labeling experiment with O_2 and $H_2{}^{18}O$, complex **1** yields benzoic acid, the ester of which shows about 15% ^{18}O incorporation (Table 3 and Figure S21c). Of note, methyl ester of benzoic acid derived from $[(Tp^{Ph2})Fe^{II}(HAP)]$[25] shows only 5% incorporation of one labeled oxygen atom from $H_2{}^{18}O$ (Figure S22 in the Supporting Information).

For complex **2**, the labeling experiment with $^{18}O_2$ supports the incorporation of both singly and doubly labeled oxygen atoms into the C−C cleavage product, adipic acid. In the ESI-mass spectrum, the ion peak at m/z 405.16 of the sodium adduct of the phenacyl ester of adipic acid shifts to 407.16 (47% ^{18}O incorporation) and 409.16 (18% ^{18}O incorporation) (Table 3 and Figure 7a,b). When the labeling experiment is carried out

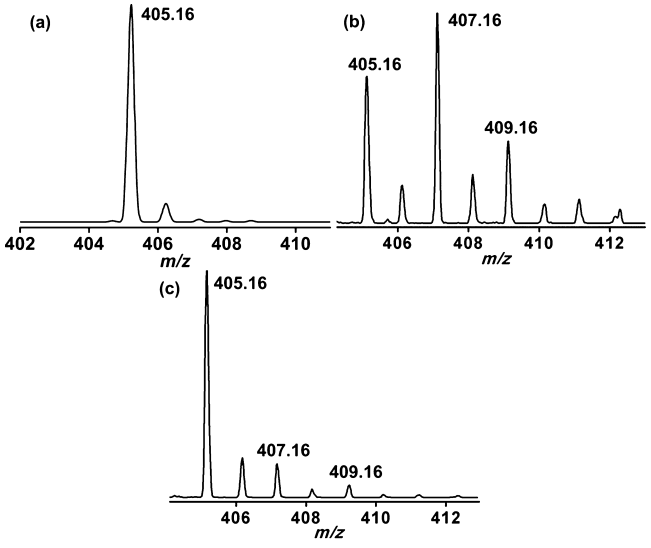

Figure 7. ESI-mass spectra of phenacyl ester of the adipic acid formed in the reaction of **2** with (a) $^{16}O_2$, (b) $^{18}O_2$, and (c) $H_2{}^{18}O$ and $^{16}O_2$.

with $^{16}O_2$ and $H_2{}^{18}O$, both singly and doubly oxygen labeled peaks are observed but with only 10% incorporation of labeled oxygen (Figure 7c).

As observed in $[(Tp^{Ph2})Fe^{II}(HAP)]$,[25] the incorporation of a labeled oxygen atom from $^{18}O_2$ into the C−C bond cleavage product is found to be low for **1** and **2** (Table 3). This low incorporation of labeled oxygen atom into carboxylic acid products indicates that a metal−oxygen intermediate species exchanges its oxygen atom with water during the reaction. The best way to verify this hypothesis is carry out labeling experiments with a system where the C−C bond cleavage product (carboxylate) remains coordinated to the iron center. Unfortunately, no ion peak corresponding to the iron species with coordinated carboxylate could be observed in the ESI-MS of the oxidized solutions of **1**−**4**. Therefore, complex **5** was used to obtain further information if solvent water is exchanged during the C−C cleavage pathway. The ion peak of the oxidized solution of the complex at m/z 509.02 is shifted to m/z 511.02 when the reaction is carried out with $^{18}O_2$ (Figure 8a).

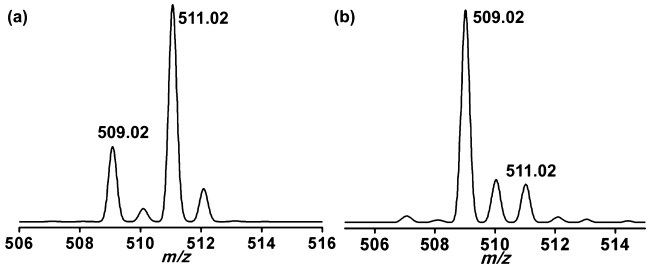

Figure 8. ESI-mass spectra (positive ion mode in acetonitrile) of the solution after oxidation of **5** with (a) $^{18}O_2$ and with (b) $H_2{}^{18}O$ and $^{16}O_2$.

This indicates that one labeled oxygen atom from $^{18}O_2$ is incorporated (70% incorporation) into benzoate. The labeling experiment with $^{16}O_2$ and $H_2{}^{18}O$ exhibits about 20% incorporation of one labeled oxygen atom from water into benzoate (Figure 8b). For complex **1** (and **2**), some loss of labeled oxygen may take place during acidic workup of the carboxylic acid product, resulting in the low level of ^{18}O incorporation from $^{18}O_2$ in the C−C bond cleavage reaction. It is important to mention here that free benzoic acid or metal-coordinated benzoate in $[(Tp^{Ph2})Fe^{II}(benzoate)]$ does not exchange its oxygen atoms with $H_2{}^{18}O$ under the experimental conditions.

In the labeling experiments with $^{18}O_2$, the two-electron-oxidized products (1,2-diketones) of α-hydroxy ketones show no incorporation of labeled oxygen atom. However, in the reaction with $^{16}O_2$ and $H_2{}^{18}O$, the diketones contain partially labeled oxygen atoms (Scheme 5). Cyclohexane-1,2-dione derived from **2**, which exhibits m/z 112 in the GC-MS, is found to contain one labeled oxygen (25% ^{18}O incorporation) from $H_2{}^{18}O$ (Figure S23 in the Supporting Information). The two-electron oxidation product of benzoin from **5**, i.e. benzil, also contains a small percentage (10%) of labeled oxygen atom from $H_2{}^{18}O$ (Figure S24 in the Supporting Information). Partial incorporation of labeled oxygen atom into the two-electron-oxidized species indicates that solvent water is

DOI: 10.1021/acs.inorgchem.5b01235
Inorg. Chem. XXXX, XXX, XXX−XXX

Scheme 5. Incorporation of Isotope-Labeled Oxygen in the Reaction of Iron(II)-α-Hydroxy Ketone Complexes with Dioxygen

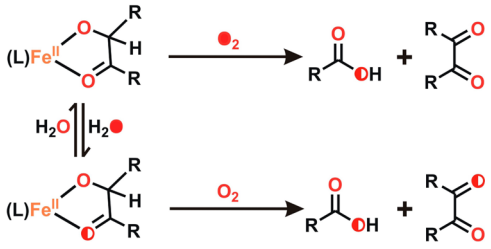

exchanged into the keto oxygen before the C−C bond cleavage step. Solvent water is known to exchange into the keto oxygen of α-hydroxy ketone.[39] Interestingly, treatment of complex **2** with $H_2{}^{18}O$ under a nitrogen atmosphere displays an ion peak two mass units higher at m/z 841.15 due to the exchange of metal-bound keto oxygen of the α-hydroxy ketone with labeled water (30% exchange with $H_2{}^{18}O$) (Figure S25 in the Supporting Information). For complex **5**, about 55% ^{18}O incorporation from $H_2{}^{18}O$ is observed under a nitrogen atmosphere (Figure S26 in the Supporting Information). Therefore, solvent water is exchanged into the keto oxygen of the coordinated α-hydroxy ketone prior to the reaction with dioxygen (Scheme 5). It should be noted that the addition of water to the iron(II) complexes has no impact on the rate of the reactions with O_2 or the product distributions.

To get an idea about the nature of metal−oxygen intermediates involved in the reaction, oxidation products from different intercepting reagents were analyzed (Scheme 6).

Scheme 6. (Top) Oxidation of External Substrates in the Reaction between Iron(II)-α-Hydroxy Ketone Complexes and Dioxygen and (Bottom) Yields of Oxidized Products from External Substrates in the Reaction with Iron(II) Complex

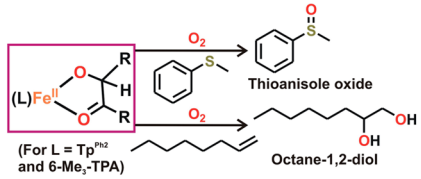

Complex	Substrate	Product	% Yield
1	Thioanisole	Thioanisole oxide	3(±1)
2	Thioanisole	Thioanisole oxide	3(±1)
3	Thioanisole	Thioanisole oxide	8(±2)
	1-Octene	Octane-1,2-diol	2(±1)
5	Thioanisole	Thioanisole oxide	9(±1)
	1-Octene	Octane-1,2-diol	5(±1)
6	Thioanisole	Thioanisole oxide	9(±1)
	1-Octene	Octane-1,2-diol	5(±1)

Similar to what was observed with $[(Tp^{Ph2})Fe^{II}(HAP)]$,[25] complex **1** oxidizes 2,4-di-*tert*-butylphenol (10 equiv) to 3,3′,5,5′-tetra-*tert*-butyl-2,2′-biphenol (DTBP). Reactions of iron(II)-α-hydroxy ketone complexes with dioxygen in the presence of thioanisole (10 equiv) afford thioanisole oxide. The yield of thioanisole oxide is found to be 2−3% with **1** and **2**, about 8% with **3**, and 9−10% with **5** and **6** (Scheme 6 and Figure S27 in the Supporting Information). A higher amount of thioanisole oxide formation corroborates the higher percentage of diketone formation with **5**. The reaction of **5** (and **6**) with 1-octene (100 equiv) yields a small amount (about 5%) of octane-1,2-diol, whereas no diol product is observed in the case of **1** and **2** (Scheme 6 and Figure S28 in the Supporting Information). Other alkene substrates such as cyclohexene and *trans*-2-heptene are not oxidized under similar experimental conditions. Importantly, external substrates have no effect on the yields of the oxidation products of α-hydroxy ketones. These results support the two-electron reduction of dioxygen on the iron(II) center with concomitant oxidation of α-hydroxy ketone to 1,2-diketone. When diketone is used as a substrate instead of α-hydroxy ketone, no C−C bond cleavage product is observed. Moreover, time-resolved experiments with complex **3** show that the yields of the diketone and carboxylic acid slowly increase over a period of 15 min (Figure S29 in the Supporting Information). Thus, diketone is not an intermediate product in the C−C bond cleavage pathway.

The iron(II)-α-hydroxy acid complexes of the Tp^{Ph2} ligand have been reported to activate dioxygen, where the metal-coordinated α-hydroxy acid anions acted as two-electron reductants (Scheme 7).[40] A nucleophilic oxidant, intercepted

Scheme 7. Reactivity of a Putative Iron(II)-Hydroperoxide Oxidant Generated in the Oxidative Decarboxylation of $[(Tp^{Ph2})Fe^{II}(benzilate)]$ Complex[40,41]

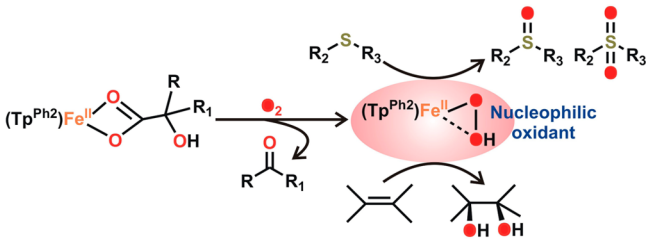

by external substrates, has been reported to exhibit versatile oxidative transformation reactions such as oxygen atom transfer to sulfides, aliphatic C−H bond activation, and olefin *cis*-dihydroxylation. On the basis of interception and mechanistic studies, the active oxidant was proposed to be a side-on iron(II)-hydroperoxide species. In the absence of any substrate, the oxidant intramolecularly hydroxylates (90%) the ortho position of one of the phenyl rings of Tp^{Ph2}.[40]

The iron(II)-α-hydroxy ketone complexes (**1**-**4**) of Tp^{Ph2} ligand react with dioxygen to exhibit C−C bond cleavage reactivity of the respective α-hydroxy ketone. In all of the cases, the C−C bond cleavage products are formed as major products. However, complex **3** exhibits a relatively higher percentage (about 20%) of 1,2-diketone formation in comparison to the other complexes (**1**, **2**, and **4**). The oxidation of α-hydroxy ketone to 1,2-diketone is a two-electron process; therefore, the amount of the iron−oxygen species corresponds to the amount of 1,2-diketone formed in the reactions. Thus, the iron−oxygen oxidant generated in the diketone formation pathway oxidizes thioanisole and 1-octene. For complex **3**, the amount of iron−oxygen oxidant may reach a value close to 20%, and as a result, formation of intramolecular oxygenated product is expected. The ESI-mass spectrum and the optical spectrum of the oxidized solution of **3** confirm the intraligand hydroxylation to an extent of about 8% (Figure S30 in the Supporting Information). Furthermore, the solution shows a rhombic EPR (X-band at 77 K) signal at g = 4.2 typical of high-spin

DOI: 10.1021/acs.inorgchem.5b01235
Inorg. Chem. XXXX, XXX, XXX−XXX

Scheme 8. Proposed Mechanism for the Oxidative C−C Bond Cleavage of α-Hydroxy Ketones on Iron Complexes

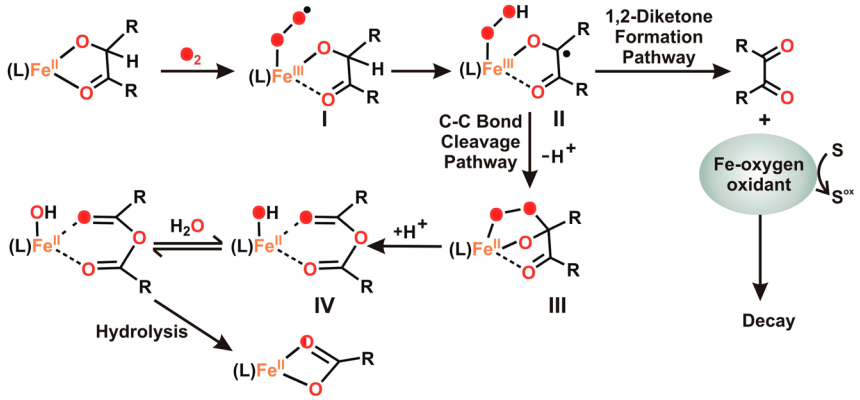

iron(III) species (Figure S30). The intraligand hydroxylation, however, gets inhibited in the presence of thioanisole (10 equiv). Thus, in analogy to that observed with the iron(II)-α-hydroxy acid complexes of the Tp^{Ph2} ligand,[40] an iron(II)-hydroperoxide species is proposed to form in the diketone formation pathway. However, in the absence of any direct experimental evidence, formation of such a species remains a proposal.

The iron(II) complexes of the tetradentate ligand afford higher percentages of 1,2-diketones. In the two-electron oxidation pathway, complex **5** is expected to form a maximum of 53% active iron−oxygen species. Although the resulting iron oxygen oxidant oxidizes thioanisole in a yield relatively higher than that observed with the tridentate ligand system, the yield of thioanisole oxide (9%) in the reaction between **5** and O_2 is low. The rest of the oxidant most likely decays to some unidentified iron species.

On the basis of the results described above, a mechanistic proposal for the C−C bond cleavage pathway of α-hydroxy ketones is put forward (Scheme 8). The reaction is initiated by activation of dioxygen at the iron(II) center to form an iron(III)-superoxide radical species (**I**). The superoxide species may either attack the carbonyl group or abstract the hydrogen atom of an α-C−H bond of the coordinated α-hydroxy ketone. In the case of nucleophilic attack of an iron(III)-superoxide, as in the mechanism of α-keto acid dependent enzymes,[42] a carbonyl compound (aldehyde or ketone) would form along with carboxylic acid product. Moreover, an iron(IV)-oxo species generated in that pathway would hydroxylate the aromatic ring to a large extent. The experimental results, however, rule out the possibility of an α-keto acid-dependent enzymelike mechanism in the C−C bond cleavage pathway of α-hydroxy ketone. Iron(III)-superoxide species are known to abstract hydrogen atom from an O−H or C−H group.[43,44] We have recently shown that the oxidative C−C bond cleavage of α-hydroxy acid was initiated via hydrogen atom abstraction from O−H bonds by an iron(III) superoxide species.[37] The hydroperoxo intermediate (**II**) releases a proton and attacks the keto carbon to generate an alkylperoxo intermediate (**III**) in the C−C bond cleavage pathway. In another pathway, intermediate **II** forms 1,2-diketone and iron(II)-oxygen oxidant (Scheme 8). Transformation of **II** to **III** is dependent on the denticity of the supporting ligand and also on the electronic properties of the coordinated α-hydroxy ketones. With the tridentate ligand, the C−C bond cleavage of the α-hydroxy ketone is the major pathway and the formation of diketone is the minor pathway. The substrate 1-(4-chlorophenyl)-2-hydroxy-2-phenylethanone (CHPE), containing an electron-withdrawing chloro substituent on the phenyl ring connected to the keto group, undergoes the oxidative C−C bond cleavage pathway only. This result supports the formation of the peroxide intermediate **III** through nucleophilic attack of the peroxide group to the keto oxygen in **II**. For the tetradentate ligand, a high percentage of **II** participates in the diketone formation pathway, which limits the yields of C−C cleavage products. In this case, one of the pyridyl arms may dissociate during the reaction that leads to the C−C bond cleavage pathway. The weakly coordinated keto oxygen of α-hydroxy ketone may also dissociate, leading to the formation of two-electron-oxidized products. Formation of the alkylperoxo intermediate **III** is proposed in the C−C bond cleavage pathway by the catechol cleaving dioxygenases and gentisate 1,2-dioxygenase.[1,45] A Baeyer−Villiger type reaction of the alkylperoxo intermediate results in O−O bond scission to generate an anhydride intermediate (**IV**). The iron(II)-hydroxide moiety of anhydride intermediate **IV** can exchange with water, which is responsible for the low incorporation of labeled oxygen into the cleavage products.

CONCLUSION

In conclusion, we have isolated a series of biomimetic iron(II)-α-hydroxy ketone complexes supported by a facial N_3 ligand and a tripodal N_4 ligand. These iron(II) complexes react with dioxygen to oxidatively cleave the aliphatic C−C bond of α-hydroxy ketones, yielding 2 equiv of carboxylic acid. In the C−C bond cleavage reaction, an oxygen atom from dioxygen is incorporated into each carboxylate unit. An iron(III)-superoxo intermediate is proposed to initiate the oxidative transformation reaction, and the C−C bond cleavage reaction follows the mechanism of an intradiol cleavage pathway. The iron complexes of the tridentate ligand afford a higher amount of C−C cleavage products in comparison to those of the tetradentate ligand, supporting the natural selection of a "3-His facial motif" in the active site of DAD. The C−C bond cleavage of α-hydroxy ketones reported in this work provides useful insight into the mechanism of oxygen-dependent transformation reaction carried out by DAD.

EXPERIMENTAL SECTION

Materials and Methods. Commercial grade chemicals were used for the synthesis and reactivity studies. *Caution!* Although no problem was encountered during the synthesis of the complexes, perchlorate salts are potentially explosive and should be handled with care.[46] The ligands KTp^{Ph2} and 6-Me_3-TPA were synthesized according to the

DOI: 10.1021/acs.inorgchem.5b01235
Inorg. Chem. XXXX, XXX, XXX−XXX

reported procedure.[47,48] Air-sensitive complexes were prepared and stored in an inert-atmosphere glovebox.

Fourier transform infrared spectroscopy on KBr pellets was performed on a Shimadzu FT-IR 8400S instrument. Elemental analyses were performed on a PerkinElmer 2400 series II CHN analyzer. Electrospray ionization mass spectra were recorded with a Waters QTOF Micro YA263 instrument. All room-temperature NMR spectra were collected on a Bruker 500 or 300 MHz spectrometer. Solution electronic spectra were recorded on an Agilent 8453 diode array spectrophotometer. GC-MS measurements were carried out with a PerkinElmer Clarus 680 GC and SQ8T MS using an Elite 5 MS (30 m × 0.25 mm × 0.25 μm) column with a maximum temperature of 300 °C. Room-temperature magnetic moment data were collected on a Gouy balance (Sherwood Scientific, Cambridge, U.K.). Diamagnetic contributions were estimated for each compound by using Pascal's constants. X-band EPR measurements were performed on a JEOL JES-FA 200 instrument. Labeling experiments were carried out with $^{18}O_2$ gas (99 atom %) or $H_2{}^{18}O$ (98 atom %) purchased from Icon Services Inc., USA.

Synthesis of Complexes. *[(Tp^{Ph2})Fe^{II}(PHAP)] (**1**).* To a methanolic (2 mL) suspension of the ligand KTp^{Ph2} (0.35 g, 0.50 mmol) was added iron(II) perchlorate hexahydrate (0.18 g, 0.50 mmol). To the suspension was added a mixture of 2-phenyl-2-hydroxyacetophenone (PHAP-H; 0.11 g, 0.50 mmol) and triethylamine (70 μL) in 1 mL of methanol with constant stirring. The mixture was stirred at room temperature for 2 h to precipitate a pink solid. The solid was filtered and washed several times with methanol. A microcrystalline solid was isolated after recrystallization of the complex from a solvent mixture of dichloromethane and methanol (1/2). Yield: 0.34 g (67%). Anal. Calcd for **1**·CH_2Cl_2 ($C_{60}H_{47}BCl_2FeN_6O_2$, 1021.62 g/mol): C, 70.54; H, 4.64; N, 8.23. Found: C, 70.48; H, 4.27; N, 8.57. IR (KBr, cm^{-1}): 3458 (br), 3061 (m), 2928 (m), 2615 (m), 1593 (s), 1545 (s), 1518 (vs), 1477 (vs), 1389 (vs), 1362 (s), 1306 (m), 1232 (m), 1171 (s), 1068 (s), 1009 (m), 918 (m), 808 (m), 760 (vs), 696 (vs), 669 (s), 526 (m). ESI-MS (positive ion mode, benzene-acetonitrile): *m/z* 725.12 ($C_{45}H_{34}BFeN_6$ expected at *m/z* 725.23) ([(Tp^{Ph2})Fe]$^+$), 743.15 ($C_{45}H_{36}BFeN_6O$ expected at *m/z* 743.24) ([(Tp^{Ph2})Fe(H$_2$O)]$^+$), 766.22 ($C_{47}H_{37}BFeN_7$ expected at *m/z* 766.26) ([(Tp^{Ph2})Fe(CH$_3$CN)]$^+$). UV−vis in benzene (*λ*, nm; *ε*, M^{-1} cm^{-1}): 515 (450), 570 (350). ^{1}H NMR (500 MHz, C_6D_6, 295 K): *δ* 52.2, 48.3, 35.5, 18.7, 18.1, 13.4, 12.9, 10.9, 8.6, 7.8, 6.0, −20.3 ppm (8 proton resonances for Tp^{Ph2} ligand and 7 proton resonances for PHAP are expected). Magnetic moment (298 K): 5.1 μ_B.

*[(Tp^{Ph2})Fe^{II}(HCH)] (**2**).* Complex **2** was synthesized according to the procedure described for complex **1**, except that 2-hydroxycyclohexanone (HCH-H) (0.06 g, 0.50 mmol) was used instead of 2-phenyl-2-hydroxyacetophenone. X-ray-quality single crystals of **2** were isolated by recrystallization of the light green solid from a dichloromethane/methanol (1/2) solvent mixture. Yield: 0.30 g (66%). Anal. Calcd for **2**·CH_3OH ($C_{53}H_{51}BFeN_6O_4$, 902.67 g/mol): C, 70.52; H, 5.69; N, 9.31. Found: C, 70.41; H, 5.86; N, 9.49. IR (KBr, cm^{-1}): 3418 (br), 3057 (m), 2932 (m), 2627 (m), 1674 (s), 1544 (s), 1479 (vs), 1462 (vs), 1414 (s), 1360 (m), 1306 (m), 1236 (m), 1169 (vs), 1070 (vs), 1008 (s), 916 (m), 810 (m), 764 (vs), 698 (vs), 669 (m), 569 (m). ESI-MS (positive ion mode, benzene-acetonitrile): *m/z* 725.12 ($C_{45}H_{34}BFeN_6$ expected at *m/z* 725.23) ([(Tp^{Ph2})Fe]$^+$), 766.22 ($C_{47}H_{37}BFeN_7$ expected at *m/z* 766.26) ([(Tp^{Ph2})Fe(CH$_3$CN)]$^+$), 839.10 ($C_{51}H_{44}BFeN_6O_2$ expected at *m/z* 839.29) ([(Tp^{Ph2})Fe(HCH) + H]$^+$), 945.10 ($C_{60}H_{46}BFeN_8$ expected at *m/z* 945.33) ([(Tp^{Ph2})Fe(3,5-diphenylpyrazole)]$^+$). UV−vis in benzene (*λ*, nm; *ε*, M^{-1} cm^{-1}): 330 (335), 380 (170). ^{1}H NMR (500 MHz, C_6D_6, 295 K): *δ* 65.0, 58.6, 52.2, 46.3, 31.6, 27.2, 24.1, 20.3, 14.1, 12.2, 11.6, 11.3,, 8.7, 6.3, −12.8, −17.3, −25.3 ppm (8 proton resonances for Tp^{Ph2} ligand and 9 proton resonances for HCH are expected). Magnetic moment (298 K): 5.3 μ_B.

*[(Tp^{Ph2})Fe^{II}(HBME)] (**3**).* Complex **3** was synthesized according to the procedure described for complex **1**, except that 2-hydroxy-1,2-bis(4-methoxyphenyl)ethanone (HBME-H; 0.14 g, 0.50 mmol) was used instead of 2-phenyl-2-hydroxyacetophenone. The pink crystalline solid of **3** was isolated by recrystallization from a dichloromethane/methanol (1/2) solvent mixture. Yield: 0.36 g (72%). Anal. Calcd for $C_{61}H_{49}BFeN_6O_4$ (996.74 g/mol): C, 73.51; H, 4.96; N, 8.43. Found: C, 73.24; H, 4.78; N, 8.67. IR (KBr, cm^{-1}): 3433 (br), 3063 (m), 2926 (m), 2623 (m), 1636 (s), 1601 (m), 1547 (s), 1475 (vs), 1410 (s), 1391 (s), 1360 (m), 1236 (m), 1171 (vs), 1070 (vs), 1011 (s), 918 (m), 814 (m), 764 (vs), 696 (vs), 671 (m), 571 (m). ESI-MS (positive ion mode, benzene-acetonitrile): *m/z* 725.23 ($C_{35}H_{34}BFeN_6$ expected at *m/z* 725.23) ([(Tp^{Ph2})Fe]$^+$), 766.29 ($C_{47}H_{37}BFeN$ expected at *m/z* 766.26) ([(Tp^{Ph2})Fe(CH$_3$CN]$^+$), 945.24 ($C_{60}H_{46}BFeN_8$ expected at *m/z* 945.33) ([(Tp^{Ph2})Fe(3,5-diphenylpyrazole)]$^+$). UV−vis in benzene (*λ*, nm; *ε*, M^{-1}cm^{-1}): 500 (585), 555 (395). ^{1}H NMR (500 MHz, C_6D_6, 295 K): *δ* 58.5, 51.8, 49.1, 35.3, 25.9, 18.9, 14.3, 13.6, 11.1, 10.6, 10.4, 8.7, 8.0, 7.6, 6.7, 4.3, −10.9, −20.9 ppm (Eight proton resonances for Tp^{Ph2} ligand and seven proton resonances for HBME are expected). Magnetic moment (298 K) = 5.1 μ_B.

*[(Tp^{Ph2})Fe^{II}(CHPE)] (**4**).* Complex **4** was synthesized according to the procedure described for complex **1**, except that 1-(4-chlorophenyl)-2-hydroxy-2-phenylethanone (CHPE-H; 0.12 g, 0.50 mmol) was used instead of 2-phenyl-2-hydroxyacetophenone. The pink crystalline solid of **4** was isolated by recrystallization from a dichloromethane/methanol (1/2) solvent mixture. Yield: 0.31 g (64%). Anal. Calcd for $C_{59}H_{44}BClFeN_6O_2$ (971.13 g/mol): C, 72.97; H, 4.57; N, 8.65. Found: C, 72.46; H, 4.34; N, 8.72. IR (KBr, cm^{-1}): 3450 (br), 3063 (m), 2926 (m), 2615 (m), 1641 (m), 1593 (s), 1547 (s), 1479 (vs), 1410 (vs), 1360 (m), 1234 (m), 1171 (vs), 1072 (vs), 1011 (m), 916 (m), 812 (m), 764 (vs), 696 (vs), 629 (m), 567 (m). ESI-MS (positive ion mode, benzene-acetonitrile): *m/z* 725.13 ($C_{35}H_{34}BFeN_6$ expected at *m/z* 725.23) ([(Tp^{Ph2})Fe]$^+$), 945.14 ($C_{60}H_{46}BFeN_8$ expected at *m/z* 945.33) ([(Tp^{Ph2})Fe(3,5-diphenylpyrazole)]$^+$), 971.21 ($C_{59}H_{45}BClFeN_6O_2$ expected at *m/z* 971.27) ([(Tp^{Ph2})Fe(CHPE) + H]$^+$). UV−vis in benzene (*λ*, nm; *ε*, M^{-1} cm^{-1}): 530 (440), 580 (360). ^{1}H NMR (500 MHz, C_6D_6, 295 K): *δ* 59.2, 52.6, 48.7, 35.6, 18.8, 18.3, 13.6, 11.0, 9.8, 9.3, 8.7, 6.8, −20.9 ppm (8 proton resonances for Tp^{Ph2} ligand and 6 proton resonances for CHPE are expected). Magnetic moment (298 K): 5.1 μ_B.

*[(6-Me$_3$-TPA)Fe^{II}(PHAP)]BPh$_4$ (**5**).* Equimolar amounts of 6-Me$_3$-TPA (0.16 g, 0.50 mmol), iron(II) perchlorate hexahydrate (0.18 g, 0.50 mmol), 2-phenyl-2-hydroxyacetophenone (PHAP-H; 0.11 g, 0.50 mmol), and triethylamine (70 μL) in 5 mL of methanol were stirred under a nitrogen atmosphere for 4 h. The solution was concentrated to 1 mL, and diethyl ether (10 mL) was added. The mixture was then stirred for another 2 h to give a brown solid of the perchlorate salt of the complex ([(6-Me$_3$-TPA)Fe^{II}(PHAP)]ClO$_4$). A methanolic solution of sodium tetraphenylborate (0.17 g, 0.50 mmol) was added to the methanolic reaction solution to precipitate a brown solid. The solid was isolated by filtration, washed with methanol, and dried. Yield: 0.28 g (61%). Anal. Calcd for $C_{59}H_{55}BFeN_4O_2$ (918.75 g/mol): C, 77.13; H, 6.03; N, 6.10. Found: C, 75.86; H, 6.01; N, 6.06. IR (KBr, cm^{-1}): 3443 (br), 3055 (s), 2924 (m), 1639 (s), 1603 (s), 1578 (s), 1452 (vs), 1254 (m), 1163 (m), 1126 (s), 1007 (m), 787 (m), 737 (vs), 704 (vs), 613 (m). ESI-MS (positive ion mode, acetonitrile): *m/z* 333.09 ($C_{21}H_{25}N_4$ expected at *m/z* 333.20) ([(6-Me$_3$-TPA) + H]$^+$), 599.09 ($C_{35}H_{35}FeN_4O_2$ expected at *m/z* 599.21) ([(6-Me$_3$-TPA)Fe(PHAP)]$^+$). UV−vis in acetonitrile (*λ*, nm; *ε*, M^{-1} cm^{-1}): 390 (1600), 560 (315). ^{1}H NMR of [(6-Me$_3$-TPA)Fe^{II}(PHAP)]ClO$_4$ (300 MHz, CD$_3$CN, 295 K): *δ* 50.7, 43.4, 23.5, 17.2, 15.9, 14.8, 14.0, 10.9, 9.7, 7.9, 6.1, −50.1 ppm (4 proton resonances for 6-Me$_3$-TPA ligand and 7 proton resonances for PHAP are expected; the methylene protons of 6-Me$_3$-TPA ligand are too broad to be observed). Magnetic moment (298 K): 4.9 μ_B.

*[(6-Me$_3$-TPA)Fe^{II}(HCH)](BPh$_4$) (**6**).* Complex **6** was synthesized according to the protocol described for **5**, except that 2-hydroxycyclohexanone (HCH-H; 0.06 g, 0.50 mmol) was used instead of 2-phenyl-2-hydroxyacetophenone. The tetraphenylborate salt of the complex was isolated upon addition of 1 equiv of sodium tetraphenylborate to the reaction solution. A deep yellow crystalline solid was obtained by recrystallization of the complex from a solvent mixture of dichloromethane and methanol (1/2). Yield: 0.27 g (66%). Anal. Calcd for $C_{51}H_{53}BFeN_4O_2$ (820.65 g/mol): C, 74.64; H, 6.51; N, 6.83. Found: C, 74.83; H, 6.23; N, 6.69. IR (KBr, cm^{-1}): 3439 (br),

DOI: 10.1021/acs.inorgchem.5b01235
Inorg. Chem. XXXX, XXX, XXX−XXX

3053 (s), 2930 (m), 2858 (m), 1672 (s), 1603 (s), 1578 (s), 1452 (vs), 1267 (m), 1155 (m), 1126 (m), 841 (m), 789 (m), 737 (vs), 706 (vs), 615 (m). UV−vis in acetonitrile (λ, nm; ε, M^{-1} cm^{-1}): 325 (1610), 390 (1575). ^{1}H NMR (500 MHz, CD_3CN, 295 K): δ 59.3, 49.9, 39.8, 35.4, 33.9, 32.3, 30.3, 20.9, 19.9, 13.3, 10.8, 7.2, 6.9, 6.8, −18.7, −23.1, −49.1 ppm (4 proton resonances for 6-Me_3-TPA ligand, 3 resonances for BPh_4 counterion, and 9 proton resonances for HCH are expected; the methylene protons of 6-Me_3-TPA ligand are too broad to be observed). Magnetic moment (298 K): 5.3 μ_B.

Reaction of Iron(II)-α-Hydroxy Ketone Complexes with Oxygen and Analysis of Organic Products. The iron(II) complex (0.02 mmol) was dissolved in 10 mL of dry organic solvent. Pure oxygen gas was bubbled through the solution for 2 min and the solution was stirred at room temperature under an oxygen environment. After the reaction (5 min for **1**, 1 h for **2**, 13 min for **3**, 10 min for **4**, 3 h for **5**, and 6 h for **6**), the solvent was removed under vacuum and the residue was treated with 10 mL of 2 M hydrochloric acid solution. The organic products were extracted with diethyl ether (3 × 15 mL) (with ethyl acetate in the case of **2** and **6**), and the organic layer was dried over anhydrous sodium sulfate. After removal of the solvent, the colorless residue was analyzed without further purification. All experiments were repeated three times to calculate the yields of oxidized products. The α-hydroxy ketone starting materials and organic products are found to be stable under acidic and aerobic conditions. Quantification of benzoic acid, benzil, and adipic acid was carried out by ^{1}H NMR integration using 1,4-benzoquinone (or 1,3,5-trimethoxybenzene) as an internal standard. In the quantification experiments, the products were analyzed immediately after workup using 1,4-benzoquinone standard. Quantification experiments were carried out in triplicate, which gave consistent results for the 1,4-benzoquinone standard. Cyclohexane-1,2-dione was quantified by GC-MS using naphthalene as an internal standard.

Ester Derivative of Benzoic Acid. The methyl ester of benzoic acid was prepared by mixing benzoic acid (isolated from the oxidized solution according to the procedure as described above) with excess diazomethane in dry diethyl ether (2 mL) at 0 °C. After the reaction solution was stirred for 5 min, the insoluble parts were separated and the clear ether layer was injected for GC-MS analysis.

Ester Derivative of Adipic Acid. Complex **2** (0.02 mmol) was dissolved in dry benzene (10 mL), and dry dioxygen gas was bubbled through the solution for 2 min. The solution was then stirred at room temperature for 1 h 15 min under an oxygen atmosphere. Acidic workup of the oxidized solution with ethyl acetate resulted in a white crude mass, which was treated with α-bromoacetophenone (0.02 mmol) and potassium fluoride (0.04 mmol) in DMF (2 mL).[49] The reaction mixture was stirred at room temperature for 24 h. The product was then extracted from the reaction mixture with diethyl ether, and the organic extract was washed several times with equal volumes of water. The organic layer was then dried over anhydrous sodium sulfate and was analyzed by ^{1}H NMR and ESI-mass spectrometry.

Interception Studies. A mixture of the iron complex (0.02 mmol) and 10 equiv of thioanisole or 100 equiv of 1-octene as intercepting agent in oxygen-saturated dry organic solvent was stirred at ambient temperature. The reaction was quenched by removing the solvent and adding 10 mL of 2 M HCl. The organic products were extracted with diethyl ether (3 × 15 mL) and characterized by ^{1}H NMR and GC-mass spectrometry. In each case, a control experiment was carried out under an oxygen atmosphere in the absence of iron complex. No product derived from the external substrate was formed in the control experiment.

X-ray Crystallographic Data Collection and Refinement of the Structure. Diffraction data of **2** were collected at 100 K on a Bruker Smart APEX II (Mo Kα radiation, λ = 0.71073 Å) instrument. Crystallographic data are provided in Table 4. Cell refinement, indexing, and scaling of the data set were carried out using the APEX2 v2.1-0 software.[50] The structures were solved by direct methods and subsequent Fourier analyses and refined by the full-matrix least-squares method based on F^2 with all observed reflections.[51] The non-hydrogen atoms were treated anisotropically. The hydrogen atoms were geometrically fixed. The unit cell contains eight disordered methanol molecules, which were treated as a diffuse contribution to the overall scattering without specific atom positions by SQUEEZE/PLATON.[52]

Table 4. Crystallographic Data for [(Tp^{Ph2})Fe^{II}(HCH)] (2)

empirical formula	$C_{51}H_{43}BFeN_6O_2$
formula wt	838.57
cryst syst	monoclinic
space group	$P2_1/c$
a, Å	14.485(7)
b, Å	19.058(9)
c, Å	16.974(8)
α, deg	90
β, deg	111.307(2)
γ, deg	90
V, Å^3	4365.6(4)
Z	4
ρ_{calcd}, Mg/m^3	1.276
T, K	100(2)
μ(Mo Kα), mm^{-1}	0.393
F(000)	1752.0
θ range, deg	2.50−23.36
no of rflns collected	51337
no. of unique rflns	7673
R(int)	0.0669
no. of data ($I > 2\sigma(I)$)	5877
no. of params refined	550
goodness of fit on F^2	1.015
R1 ($I > 2\sigma(I)$)	0.0489
wR2	0.1420

■ ASSOCIATED CONTENT

Supporting Information

The Supporting Information is available free of charge on the ACS Publications website at DOI: 10.1021/acs.inorgchem.5b01235.

All spectral data (PDF)
X-ray crystallographic data (CIF)

■ AUTHOR INFORMATION

Corresponding Author

*T.K.P.: e-mail, ictkp@iacs.res.in; fax, +91-33-2473-2805; tel, +91-33-2473-4971.

Notes

The authors declare no competing financial interest.

■ ACKNOWLEDGMENTS

T.K.P. gratefully acknowledges the Indian National Science Academy for financial support (Project for INSA Young Scientist Awardee). R.R. thanks the Council of Scientific and Industrial Research (CSIR), India, for a research fellowship. X-ray diffraction data of the complex were collected at the DST-funded National Single Crystal Diffractometer Facility at the Department of Inorganic Chemistry, Indian Association for the Cultivation of Science.

■ REFERENCES

(1) Fetzner, S. *Appl. Environ. Microbiol.* **2012**, *78*, 2505−2514.
(2) Allpress, C. J.; Berreau, L. M. *Coord. Chem. Rev.* **2013**, *257*, 3005−3029.

DOI: 10.1021/acs.inorgchem.5b01235
Inorg. Chem. XXXX, XXX, XXX−XXX

(3) Gaido, K. W.; Leonard, L. S.; Lovell, S.; Gould, J. C.; Babai, D.; Portier, C. J.; McDonnell, D. P. *Toxicol. Appl. Pharmacol.* **1997**, *143*, 205−212.
(4) Timms, B. G.; Howdeshell, K. L.; Barton, L.; Bradley, S.; Richter, C. A.; vom Saal, F. S. *Proc. Natl. Acad. Sci. U. S. A.* **2005**, *102*, 7014−7019.
(5) Lobos, J. H.; Leib, T. K.; Su, T.-M. *Appl. Environ. Microbiol.* **1992**, *58*, 1823−1831.
(6) Sasaki, M.; Akahira, A.; Oshiman, K.; Tsuchido, T.; Matsumura, Y. *Appl. Environ. Microbiol.* **2005**, *71*, 8024−8030.
(7) Spivack, J.; Leib, T. K.; Lobos, J. H. *J. Biol. Chem.* **1994**, *269*, 7323−7329.
(8) Hopper, D. J.; Elmorsi, E. A. *Biochem. J.* **1984**, *218*, 269−72.
(9) Hopper, D. J.; Jones, H. G.; Elmorsi, E.; Rhodes-Roberts, M. E. *Microbiology* **1985**, *131*, 1807−14.
(10) Hopper, D. J. *Biochem. J.* **1986**, *239*, 469−72.
(11) Hopper, D. J.; Kaderbhai, M. A. *Biochem. J.* **1999**, *344*, 397−402.
(12) Enya, M.; Aoyagi, K.; Hishikawa, Y.; Yoshimura, A.; Mitsukura, K.; Maruyama, K. *Biosci., Biotechnol., Biochem.* **2012**, *76*, 567−574.
(13) Berreau, L. M.; Borowski, T.; Grubel, K.; Allpress, C. J.; Wikstrom, J. P.; Germain, M. E.; Rybak-Akimova, E. V.; Tierney, D. L. *Inorg. Chem.* **2011**, *50*, 1047−1057.
(14) Siewert, I.; Limberg, C. *Angew. Chem., Int. Ed.* **2008**, *47*, 7953−7956.
(15) Allpress, C. J.; Miłaczewska, A.; Borowski, T.; Bennett, J. R.; Tierney, D. L.; Arif, A. M.; Berreau, L. M. *J. Am. Chem. Soc.* **2014**, *136*, 7821−7824.
(16) Szajna, E.; Arif, A. M.; Berreau, L. M. *J. Am. Chem. Soc.* **2005**, *127*, 17186−17187.
(17) Paine, T. K.; England, J.; Que, L., Jr. *Chem. - Eur. J.* **2007**, *13*, 6073−6081.
(18) Siewert, I.; Limberg, C.; Demeshko, S.; Hoppe, E. *Chem. - Eur. J.* **2008**, *14*, 9377−9388.
(19) Schröder, K.; Join, B.; Amali, A. J.; Junge, K.; Ribas, X.; Costas, M.; Beller, M. *Angew. Chem., Int. Ed.* **2011**, *50*, 1425−1429.
(20) Kaizer, J.; Baráth, G.; Pap, J.; Speier, G.; Giorgi, M.; Réglier, M. *Chem. Commun.* **2007**, 5235−5237.
(21) Kitajima, N.; Amagai, H.; Tamura, N.; Ito, M.; Moro-oka, Y.; Heerwegh, K.; Penicaud, A.; Mathur, R.; Reed, C. A.; Boyd, P. D. W. *Inorg. Chem.* **1993**, *32*, 3583−3584.
(22) Sun, Y.-J.; Huang, Q.-Q.; Zhang, J.-J. *Inorg. Chem.* **2014**, *53*, 2932−2942.
(23) Park, H.; Bittner, M. M.; Baus, J. S.; Lindeman, S. V.; Fiedler, A. T. *Inorg. Chem.* **2012**, *51*, 10279−10289.
(24) Bowyer, A. Ph.D. Thesis, University of Southampton, 2008.
(25) Paria, S.; Halder, P.; Paine, T. K. *Angew. Chem., Int. Ed.* **2012**, *51*, 6195−6199.
(26) Chen, J.; Li, W.; Wang, M.; Zhu, G.; Liu, D.; Sun, F.; Hao, N.; Li, X.; Rao, Z.; Zhang, X. C. *Protein Sci.* **2008**, *17*, 1362−1373.
(27) Beaven, G.; Bowyer, A.; Erskine, P.; Wood, S. P.; McCoy, A.; Coates, L.; Keegan, R.; Lebedev, A.; Hopper, D. J.; Kaderbhai, M. A.; Cooper, J. B. *Acta Crystallogr., Sect. F: Struct. Biol. Commun.* **2014**, *70*, 823−826.
(28) Keegan, R.; Lebedev, A.; Erskine, P.; Guo, J.; Wood, S. P.; Hopper, D. J.; Rigby, S. E. J.; Cooper, J. B. *Acta Crystallogr., Sect. D: Biol. Crystallogr.* **2014**, *70*, 2444−2454.
(29) Chiou, Y.-M.; Que, L., Jr. *J. Am. Chem. Soc.* **1995**, *117*, 3999−4013.
(30) Wistuba, T.; Limberg, C.; Pritzkow, H. *Z. Anorg. Allg. Chem.* **2002**, *628*, 2340−2344.
(31) Lewiński, J.; Justyniak, I.; Ochal, Z.; Zachara, J. *J. Chem. Soc., Dalton Trans.* **1999**, 2909−2911.
(32) Ahn, H. S.; Davenport, T. C.; Tilley, T. D. *Chem. Commun.* **2014**, *50*, 3834−3837.
(33) Weinert, C. S.; Fenwick, A. E.; Fanwick, P. E.; Rothwell, I. P. *Dalton Trans.* **2003**, 532−539.
(34) Wistuba, T.; Limberg, C.; Kircher, P. *Angew. Chem., Int. Ed.* **1999**, *38*, 3037−3039.
(35) Addison, A. W.; Rao, T. N.; Reedijk, J.; van Rijn, J.; Verschoor, G. C. *J. Chem. Soc., Dalton Trans.* **1984**, 1349−1356.
(36) Mehn, M. P.; Fujisawa, K.; Hegg, E. L.; Que, L., Jr. *J. Am. Chem. Soc.* **2003**, *125*, 7828−7842.
(37) Paria, S.; Que, L., Jr.; Paine, T. K. *Angew. Chem., Int. Ed.* **2011**, *50*, 11129−11132.
(38) Kim, J.; Zang, Y.; Costas, M.; Harrison, R. G.; Wilkinson, E. C.; Que, L., Jr. *JBIC, J. Biol. Inorg. Chem.* **2001**, *6*, 275−284.
(39) Bunton, C. A.; Shiner, V. J., Jr. *J. Chem. Soc.* **1960**, 1593−1598.
(40) Paria, S.; Chatterjee, S.; Paine, T. K. *Inorg. Chem.* **2014**, *53*, 2810−2821.
(41) Chatterjee, S.; Paine, T. K. *Angew. Chem., Int. Ed.* **2015**, *54*, 9338−9342.
(42) Martinez, S.; Hausinger, R. P. *J. Biol. Chem.* **2015**, *290*, 20702−20711.
(43) Paine, T. K.; Paria, S.; Que, L., Jr. *Chem. Commun.* **2010**, *46*, 1830−1832.
(44) Mukherjee, A.; Cranswick, M. A.; Chakrabarti, M.; Paine, T. K.; Fujisawa, K.; Münck, E.; Que, L., Jr. *Inorg. Chem.* **2010**, *49*, 3618−3628.
(45) Bugg, T. D. H.; Lin, G. *Chem. Commun.* **2001**, *11*, 941−953.
(46) Wolsey, W. C. *J. Chem. Educ.* **1973**, *50*, A335−A337.
(47) Kitajima, N.; Fujisawa, K.; Fujimoto, C.; Moro-oka, Y.; Hashimoto, S.; Kitagawa, T.; Toriumi, K.; Tatsumi, K.; Nakamura, A. *J. Am. Chem. Soc.* **1992**, *114*, 1277−1291.
(48) Britovsek, G. J. P.; England, J.; White, A. J. P. *Inorg. Chem.* **2005**, *44*, 8125−8134.
(49) Clark, J. H.; Miller, J. M. *Tetrahedron Lett.* **1977**, *18*, 599−602.
(50) *APEX 2 v2.1-0*; Bruker AXS, Madison, WI, 2006.
(51) Sheldrick, G. M. *SHELXL-97, Program for Crystal Structure Analysis (Release 97-2)*; University of Göttingen, Göttingen, Germany, 1998.
(52) Spek, A. L. *PLATON. A Multipurpose Crystallographic Tool*; Utrecht University, Utrecht, The Netherlands, 2002.

DOI: 10.1021/acs.inorgchem.5b01235
Inorg. Chem. XXXX, XXX, XXX−XXX